

01,07,11

## Influence of high pressures on the formation of new phase in the $\text{Al}_{86}\text{Ni}_2\text{Co}_6\text{Gd}_6$ alloy

© S.G. Menshikova<sup>1</sup>, V.V. Brazhkin<sup>2</sup>

<sup>1</sup> Udmurt Federal Research Center, Ural Branch Russian Academy of Sciences, Izhevsk, Russia

<sup>2</sup> Institute for High Pressure Physics, Russian Academy of Sciences, Moscow, Troitsk, Russia

E-mail: svetlmenh@mail.ru

Received July 8, 2021

Revised July 13, 2021

Accepted July 16, 2021

The structure, elemental and phase composition of the eutectic alloy  $\text{Al}_{86}\text{Ni}_2\text{Co}_6\text{Gd}_6$  (hereinafter referred to as at.%) During the solidification of the melt from 1500°C at a rate of 1000°C/s under high pressure of 3 and 7 GPa have been investigated by X-ray diffraction analysis and electron microscopy. Solidification of the melt under high pressure leads to a change in the phase composition of the alloy and the formation of an anomalously supersaturated solid solution of  $\alpha\text{-Al}(\text{Gd})$ . At a pressure of 7 GPa, new phases were synthesized:  $\text{Al}_3\text{Gd}^*$  (like  $\text{Al}_3\text{U}$ ) containing Co and Ni, with a primitive cube structure (cP4/2) with a lattice parameter  $a = 4.285 \pm 0.002$  Angstrom and  $\text{Al}_8\text{Co}_4\text{Gd}^*$  (like  $\text{Al}_8\text{Cr}_4\text{Gd}$ ) with a tetragonal structure (tI26/1) with parameters  $a = 8.906 \pm 0.003$  Angstrom and  $c = 5.150 \pm 0.003$  Angstrom. The structure of all the samples obtained is homogeneous, dense, finely dispersed, without shrinkage cavities and pores. The average microhardness of the samples is high due to solid solution and precipitation hardening.

**Keywords:** high pressure, microstructure, phase, microhardness, melt.

DOI: 10.21883/PSS.2022.02.54003.32s

### 1. Introduction

The engineering of materials with the required structure and properties at known thermodynamic parameters (temperature, pressure, and chemical composition) is one of the primary and most pressing issues in condensed-matter physics and chemistry. Aluminum-based multicomponent glass-forming alloys of the Al-TM-REM type (TM is a transition metal and REM is a rare-earth metal) are viable for practical application as structural materials. Such alloys containing REMs paired with 3d metals feature fine mechanical properties and high thermal stability. A combination of various extreme factors (ultrafast and fast cooling from melt, ultrahigh and high pressures and temperatures, ultrastrong and strong electric and magnetic fields, etc.) provides an opportunity to expand the regions of metastable states, synthesize new compounds and new modifications of known compounds, and modify the defect structure at micro- and nanolevels (i.e., obtain materials with various types of structure (amorphous, quasi- and nanocrystalline) and, consequently, different properties [1,2]). Combined with fast cooling ( $10^3\text{--}10^5\text{C/s}$ ), high pressure (several GPa) facilitates the synthesis of new structures and serves as a universal parameter of study of the nature of chemical bonding and atomic interactions. It is known that high pressures may induce various changes in the structure of alloys

(depending on the initial state of these alloys): separation of an initially homogeneous amorphous phase and formation of stable and metastable phases [3–5]. Pressure affects the structure of metals and alloys in the process of solidification; it enhances their properties by enlarging the crystallization nuclei and reducing the size of micropores and inhibits the formation of shrinkage cavities. When a melt is subjected to fast solidification under high pressure, it is reasonable to expect an enhancement of mutual solubility of components, fragmentation and diminution of grains, changes in the crystallization mechanism, etc. [6,7].

Several glass-forming phases may emerge in alloys of the Al-TM-REM type [1,8,9]. The competition between these nucleating phases results in the formation of metastable phases and contributes to an increase in the amorphization ability of alloys. The aim of the present study is to investigate the possibility of formation of new phases in the  $\text{Al}_{86}\text{Ni}_2\text{Co}_6\text{Gd}_6$  alloy in the process of fast solidification of its high-temperature melt under high pressure.

### 2. Materials and research techniques

An ingot of the  $\text{Al}_{86}\text{Ni}_2\text{Co}_6\text{Gd}_6$  composition was produced by fusing metals in alumina crucibles in a Tammann furnace. The initial components were elements with the following base metal content: aluminum — 99.999, nickel — 99.93, cobalt — 99.99, and gadolinium — 99.9 wt.%.

\* Report at XXI All-Russian School-Seminar on Problems of Condensed Matter Physics (SPCMP-21), Yekaterinburg, March 18–25, 2021

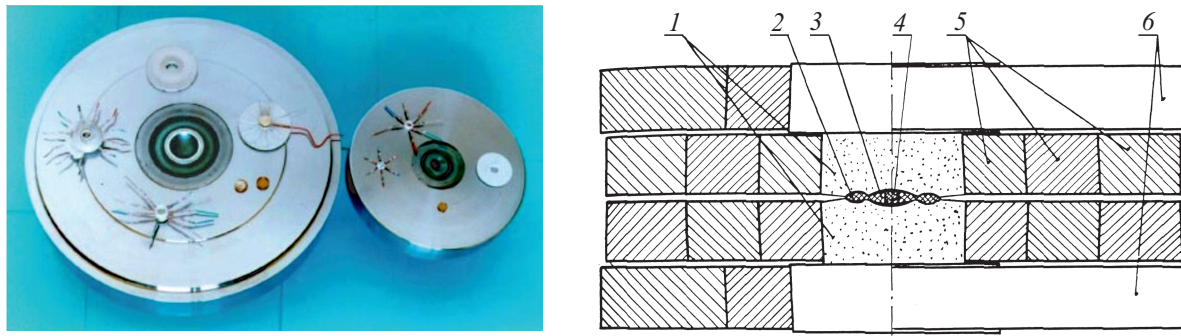


**Figure 1.** Toroid-type chamber. 1 — solid alloy, 2 — torus, 3 — central region in the form of a lens, 4 — heater and sample, 5 — steel rings, 6 — support plates.

The alloying technology was as follows: heating Al to 800°C

→ introducing Ni, Co (raising the temperature to 1050°C within 50 min) → stirring with an alumina rod at 1050°C; → cooling to 850°C → introducing the entire amount of Gd (heating within 15 min to 1020°C) → stirring with an alumina rod → tapping into a cast-iron mold with  $d \sim 21$  mm.

The ingot was then remelted two times in a vacuum furnace to make the distribution of alloying elements more uniform. The results of chemical analysis of the ingot revealed that the concentration of base components corresponded (within  $\pm 0.25\%$ ) to the nominal composition. This ingot was regarded as the initial sample.

Samples for study were prepared under high pressures (3 and 7 GPa) in a toroid-type high-pressure chamber [10] (Fig. 1). This chamber was formed by plane anvils (made of a hard alloy) pressed into steel rings. Catlenite (Algeti stone) served as a pressure-transmitting medium. The basic principle of pressurization in a chamber of this design is the alternation of compression and outflow of the pressure-transmitting medium. The studied samples were compressed by pressure stamps made of a hard alloy. An annular gap between these stamps was provided for the outflow of solid matter. The outflow ceases after an equilibrium between the forces of pressure in the central region of the chamber and friction in the annular gap is established. When the load is increased further, the pressure rises only due to the compression of the solid medium. The use of the solid pressure-transmitting medium instead of a liquid or gaseous one provides an opportunity to raise both the pressure and the temperature in experiments. The values of pressure were chosen with consideration of the results of earlier studies of other alloys of the Al-TM-REM type (80–90 at.% Al) [11–13].

Melts were cooled at a rate of 1000°C/s, the melt temperature prior to quenching was 1500°C. Heating and melting were performed by passing alternating current through a sample introduced into a crucible made of hexagonal boron nitride. High-pressure stamps served as current leads. The temperature value was calculated based on the thyristor readings (current passed through a

sample). The pressure was kept constant throughout the entire experiment. Following cooling of a sample to room temperature, the pressure was reduced to atmospheric pressure. The phase composition of samples was determined by X-ray diffraction analysis using Dron-6 ( $\text{CuK}\alpha$  radiation) and Dron-3 ( $\text{CoK}\alpha$  radiation) diffractometers. The  $2\theta$  measurement range was 20–120°, the angle pitch was 0.05°, and the exposure time was 20 s. The measurement mode was chosen so as to achieve an accuracy sufficient to determine the angular position of diffraction maxima and the total intensity. The PHAN software from the MIS&A package and the „Topaz“ program were used to process the obtained XRD patterns (determine the phase composition, lattice parameters, and the space group of phases). The profiles of XRD patterns of the studied samples were loaded into these programs, processed, and analyzed. A QuattroS system (scanning electron microscope (SEM) with a standard ABS/CBS directional backward scattering detector) system was used to determine the chemical and elemental composition, the morphology, and the size of structural components of the alloy. The error of determination of the percentage of elements in samples was no higher than 5%. The analysis of structure was performed in high- and low-vacuum modes. The high-vacuum mode is the standard mode of SEM operation. The low-vacuum mode is the natural environment mode. A three-stage vacuum system was used: preliminary vacuum, vacuum in the chamber, and vacuum in the source region were maintained by a forevacuum pump (pre-vacuum pump, PVP), a turbo molecular pump (TMP), and an ion getter pump (IGP), respectively. In the low-vacuum mode, the electron column was under high vacuum, and auxiliary gas under pressure was in the sample chamber. The convergence of the SEM and X-ray detection (specifically, energy-dispersive X-ray spectroscopy, EDX) system within a short working distance allowed us to perform high-accuracy chemical analysis with high resolution of surface and subsurface characteristics. Durametric measurements (Vickers hardness  $H_v$ ) were performed using a PMT-3M microhardness tester with a load of 50 g and an exposure time of 10 s. The values of  $H_v$  were averaged over 20 measurements.

**Table 1.** Synthesis conditions and phase composition of Al<sub>86</sub>Ni<sub>2</sub>Co<sub>6</sub>Gd<sub>6</sub> samples

№	Synthesis conditions	Phase composition
1	Initial sample	$\alpha$ -Al(Gd) (cub., cF4/1), Al <sub>9</sub> Co <sub>2</sub> (monocl., mP22/1), Al <sub>3</sub> Gd (hex., hP8/3), Al <sub>3</sub> Ni (orthor., oP16/2)
2	3 GPa (1500°C)	$\alpha$ -Al(Gd) (cub., cF4/1), Al <sub>4</sub> CoNi <sub>2</sub> (cub., cI112/1)
3	7 GPa (1500°C)	$\alpha$ -Al(Gd) (cub., cF4/1), Al <sub>3</sub> Gd*(Ni/Co) (Al <sub>3</sub> U-type) (cub., cP4/2), Al <sub>8</sub> Co <sub>4</sub> Gd** (Al <sub>8</sub> Cr <sub>4</sub> Gd-type) (tetr., tI26/1)

### 3. Results and discussion

Table 1 presents the synthesis conditions and the phase composition (determined by X-ray diffraction analysis) of the initial sample of the studied alloy and samples produced under high pressure. The microstructure (under different magnification) and the concentration maps of alloying element (Ni, Co, Gd) distribution in the samples are shown in Fig. 2. The results of semiquantitative elemental analysis of the structural components of samples are listed in Tables 2–4.

Figure 2, *a* presents the microstructure of the initial Al<sub>86</sub>Ni<sub>2</sub>Co<sub>6</sub>Gd<sub>6</sub> ingot. Large primary crystals of phase Al<sub>3</sub>Gd in the form of platelets thicker than 20  $\mu$ m of various length (white crystals in Fig. 2, *a*), solid solution  $\alpha$ -Al(Gd) with 0.51% of Gd (black regions in Fig. 2, *a* with a size on the order of 5  $\mu$ m, phase Al<sub>9</sub>Co<sub>2</sub> (gray phase in Fig. 2, *a*), and a small amount of phase Al<sub>3</sub>Ni (light gray thin needle-like crystals in Fig. 2, *a* with a length on the order of 10  $\mu$ m) are present in the structure. The remaining space is filled with an irregular disperse lamellar-rod eutectic with the following elemental composition: Al<sub>80.41%</sub>Ni<sub>3.16%</sub>Co<sub>14.78%</sub>Gd<sub>1.65%</sub> (see Table 2). This eutectic is located primarily within phases Al<sub>3</sub>Gd and Al<sub>9</sub>Co<sub>2</sub> (Fig. 2, *a*).

The phase composition of the alloy changes in the process of solidification under a pressure of 3 GPa. The alloy crystallizes with the formation of two equilibrium phases:  $\alpha$ -Al(Gd) and Al<sub>4</sub>CoNi<sub>2</sub> (see Table 1). Thin rod-like crystals of phase Al<sub>4</sub>CoNi<sub>2</sub> with a length of  $\sim$ 100  $\mu$ m and a thickness lower than 5  $\mu$ m form first (Fig. 2, *b*). These crystals contain elements of the Al<sub>70.33</sub>Ni<sub>22.96</sub>Co<sub>6.71</sub> alloy (see Table 3). The growth of dendrites of phase  $\alpha$ -Al originates from the primary crystals (Fig. 2, *b*). The concentration of Gd in  $\alpha$ -Al (1.5%) is almost three times higher than its concentration in the initial sample. Since rare-earth metals are characterized by relatively large atom sizes, they do not form major regions of solubility with other metals in the solid state; the solubility also does not increase significantly with temperature. REMs are infinitely soluble with each other in both liquid and solid states. Presumably, high pressure plays a leading part in the formation of an anomalously supersaturated solution. An irregular lamellar-rod eutectic ( $\alpha$ -Al(Gd)+ and Al<sub>4</sub>CoNi<sub>2</sub>) forms

**Table 2.** Elemental analysis of the initial sample Al<sub>86</sub>Ni<sub>2</sub>Co<sub>6</sub>Gd<sub>6</sub>

Element	at.%			
	Al <sub>3</sub> Gd	$\alpha$ -Al(Gd)	Al <sub>9</sub> Co <sub>2</sub>	Eutectic
Al	76.12	99.49	82.12	80.41
Ni	–	–	–	3.16
Co	–	–	17.88	14.78
Gd	23.88	0.51	–	1.65

**Table 3.** Elemental analysis of sample Al<sub>86</sub>Ni<sub>2</sub>Co<sub>6</sub>Gd<sub>6</sub> (3 GPa, 1500°C)

Element	at.%		
	Al <sub>4</sub> CoNi <sub>2</sub>	$\alpha$ -Al(Gd)	Eutectic
Al	70.33	98.50	91.21
Ni	22.96	–	1.40
Co	6.71	–	3.14
Gd	–	1.50	4.24

**Table 4.** Elemental analysis of sample Al<sub>86</sub>Ni<sub>2</sub>Co<sub>6</sub>Gd<sub>6</sub> (7 GPa, 1500°C)

Element	at.%			
	Al <sub>3</sub> Gd*(Ni/Co)	$\alpha$ -Al(Gd)	Coarse eutectic	Fine eutectic
Al	75.38	98.90	90.95	91.66
Ni	2.47	–	1.39	–
Co	15.62	–	5.22	1.73
Gd	6.17	1.10	2.45	6.61

next (Fig. 2, *b*). In general, the structure is substantially finer than the one in the initial sample.

The examination of the sample obtained by cooling the melt under a pressure of 7 GPa revealed that the phase composition of the alloy changes just as it did in the case of 3 GPa (see Table 1), although new phases and formations of a complex geometric shape emerge. The ingot has a crystalline finely dispersed structure. Compared to the initial sample, the structure is refined so that the size of primary crystals becomes comparable to the eutectic size. Figure 3 shows the X-ray diffraction pattern of the

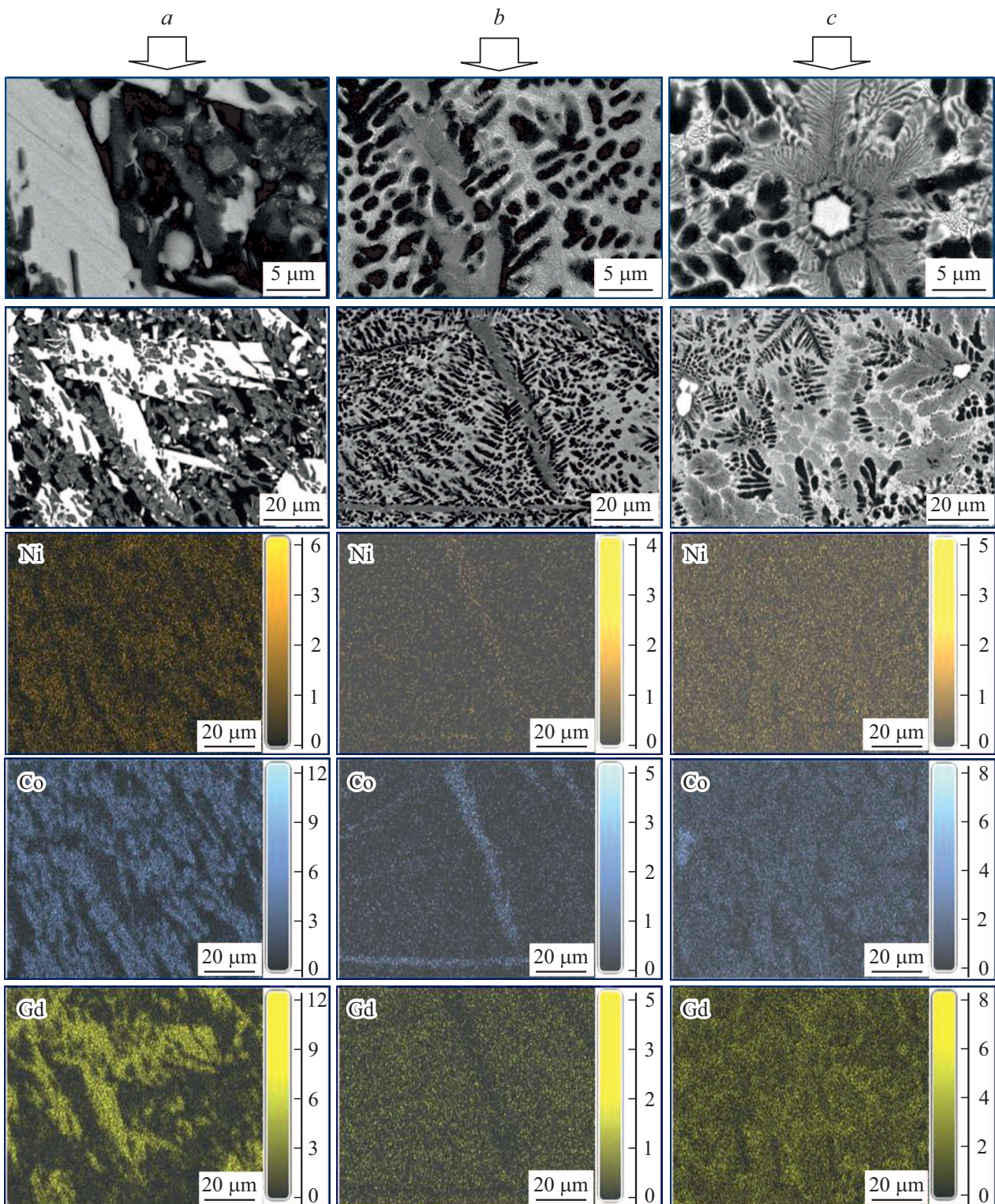


**Figure 2.** Microstructure of samples  $\text{Al}_{86}\text{Ni}_2\text{Co}_6\text{Gd}_6$  under different magnification and concentration maps of element distribution in the samples: initial sample (a), 3 GPa (b), 7 GPa (c).

sample. The melt crystallizes in stages. At the first stage, phase  $\text{Al}_3\text{Gd}^*(\text{Ni}, \text{Co})$  of the  $\text{Al}_3\text{U}$  type forms based on the  $\text{Al}_3\text{Gd}$  compound (white crystals in Fig. 2, c); in addition to Gd, this phase contains Ni and Co. The percentage of

elements in it is as follows:  $\text{Al}_{75.38\%}\text{Ni}_{2.47\%}\text{Co}_{15.62\%}\text{Gd}_{6.17\%}$ . It was found that this phase has the structure of a primitive cube ( $cP4/2$ ) with lattice parameter  $a = 4.285 \pm 0.002 \text{ \AA}$ . Known equilibrium phase  $\text{Al}_3\text{Gd}$  has a hexagonal lattice,

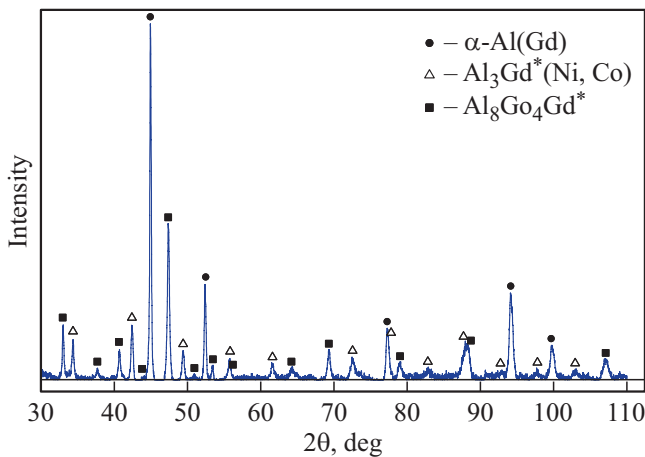


**Figure 3.** X-ray diffraction pattern of the  $\text{Al}_{86}\text{Ni}_2\text{Co}_6\text{Gd}_6$  alloy (7 GPa, 1500°C).

and equilibrium phase  $\text{Al}_2\text{Gd}$ , which is close to  $\text{Al}_3\text{Gd}$ , has a cubic lattice, but it does not manifest itself in the diffraction pattern. Apparently, a nonequilibrium version of phase  $\text{Al}_3\text{Gd}$  was obtained. If the growth conditions are favorable, crystals of this phase tend to form compact, regular, homogeneous, and isotropic hexagons  $\sim 5\ \mu\text{m}$  in size or assume the shape of a symmetric isotropic dendrite with well-developed branches that form petals (Fig. 2, c). Crystal growth sites may have slightly different temperature regimes, flow regimes of the feed solution, etc. Therefore, depending on the state of the melt, crystals grow both in length and in width due to the concentration, temperature, and chemical nonuniformity and assume various forms: the form close to a quasicrystal with a fifth-order symmetry axis and the form of slightly elongated columns with six-ray symmetry at the base (when growth proceeds primarily along the crystal axis). Hexagonal platelets or hexagonal stars form in the case of growth in directions perpendicular to the crystal axis. The faces of a growing crystal are covered with a thin liquid film of the so-called quasi-liquid layer. This phenomenon is related to surface „melting“ that is observed on the surface of a number of crystalline materials and is a variation of the first-order phase transition. The mentioned „melting“ occurs at temperatures below the alloy melting point due to the fact that the bonds of atoms on the crystal surface are less strong than the bonds of atoms in the bulk. This effect governs the chemical interactions between melt atoms on the surface of a crystal and the processes of its growth. The arrangement of atoms in the melt structure before quenching predetermines the form of crystal growth and the crystal symmetry. It is reasonable to assume that clusters forming in the melt under high pressure tend to have a denser packing than those forming under atmospheric pressure. Anomalous supersaturated solid solution  $\alpha\text{-Al(Gd)}$  forms next (black regions in Fig. 2, c). The concentration of Gd in the solid solution is two times higher than its concentration in the initial sample. Phase  $\alpha\text{-Al(Gd)}$  is represented by finely branched dendrites that

grow radially from the primary crystals. Primary and secondary branches with marked anisotropy of their growth rate are seen clearly in Fig. 2, c. The lines of this phase in the diffraction spectrum are shifted somewhat toward lower angles  $2\theta$ . A spherulitic eutectic forms after the primary crystals and the  $\alpha$ -phase: fan-shaped splitting of a platelet packet is seen clearly in Fig. 2, c. Such nonequilibrium growth forms as spherulites or globules emerge due to high supercooling at the melt crystallization front [14]. All elements of the alloy are found in the eutectic (see Table 4). Thus, it is fair to assume that the eutectic is a mixture of phase  $\alpha\text{-Al(Gd)}$  and nonequilibrium phase  $\text{Al}_3\text{Gd}^*(\text{Ni, Co})$ . Each eutectic colony grows from its own center. The nucleation of a colony is initiated by the basic phase characterized by a greater fraction of directed interatomic bonds (i.e., phase  $\text{Al}_3\text{Gd}^*(\text{Ni, Co})$ ). The second eutectic phase,  $\alpha\text{-Al(Gd)}$ , grows on the basic one as on a substrate. An irregular lamellar-rod eutectic forms in the remaining space (Fig. 2, c). It contains Al, Co, and Gd, which form a mixture of phases ( $\alpha\text{-Al(Gd)} + \text{Al}_8\text{Co}_4\text{Gd}^*$ ). Phase  $\text{Al}_8\text{Co}_4\text{Gd}^*$  is ordered in the same way as known phase  $\text{Al}_8\text{Cr}_4\text{Gd}$ , but the lines of the obtained phase in the diffraction spectrum are shifted somewhat toward higher angles  $2\theta$ . Phase  $\text{Al}_8\text{Co}_4\text{Gd}^*$  has a tetragonal structure (tI26/1) with lattice parameters  $a = 8.906 \pm 0.003$  and  $c = 5.150 \pm 0.003$  Å. Thus, the chosen conditions set such kinetics of nucleation and growth of crystallization center phases that correspond to the emergence of a disperse structure containing metastable formations.

The structure of samples formed under pressure is homogeneous and dense; shrinkage cavities and pores were not observed. It was found that the sample formed under a pressure of 7 GPa has high average microhardness ( $\sim 1700$  MPa) due to solid-solution and precipitation hardening. This value is almost two times higher than the microhardness of the initial sample.

## 4. Conclusion

The combination of a high solidification rate and mechanical compaction under high pressure provided an opportunity to produce alloys with a refined structure and high density. The average microhardness of samples formed under pressure is high due to solid-solution and precipitation hardening. New crystalline phases form under a pressure of 7 GPa:  $\text{Al}_3\text{Gd}^*$  ( $\text{Al}_3\text{U}$ -type), which contains Co and Ni, with the structure of a primitive cube (cP4/2) and  $\text{Al}_8(\text{Ni/Co})_4\text{Gd}^*$  ( $\text{Al}_8\text{Cr}_4\text{Gd}$ -type) with a tetragonal structure (tI26/1). An anomalously supersaturated solution  $\alpha\text{-Al(Gd)}$  also forms. Thus, new high-pressure phases with their region of thermodynamic stability corresponding to the high-pressure region were obtained. High-pressure phases of the  $\text{Al}_3\text{P3M}^*$  type have already been synthesized under the same conditions in alloys  $\text{Al}_{90}\text{Y}_{10}$ ,  $\text{Al}_{87}\text{Ni}_8\text{Y}_5$ , and  $\text{Al}_{86}\text{Ni}_6\text{Gd}_4\text{Tb}_2\text{Er}_2$  [11–13]. It is evident that the obtained new phases warrant further thorough study.

The presented results demonstrate that it is technically possible to alter the properties of industrial aluminum alloys without changing their chemical composition by applying the method of solidification under pressure, thus modifying the structure and the chemical composition of structural components of the sample.

### Acknowledgments

Electron microscopic studies were performed at the „Center for Physical and Physico-Chemical Methods of Analysis and Study of Properties and Characteristics of Surfaces, Nanostructures, Materials, and Products“ of the Udmurt Federal Research Center of the Ural Branch of the Russian Academy of Sciences (Izhevsk).

The authors would like to thank I.K. Averkiev for his help in elemental analysis of samples and Cand. Sci. (Phys.–Math.) V.A. Volkov for his help in X-ray diffraction analysis.

### Funding

This study was carried out under state assignment of the Ministry of Science and Higher Education of the Russian Federation (project No. 121030100001-3).

### Conflict of interest

The authors declare that they have no conflict of interest.

### References

- [1] I. Inoue. *Prog. Mater. Sci.* **43**, 365 (1998).
- [2] A.M. Glezer, N.A. Shurygina. *Amorfno-nanokristallicheskie splavy*. Fizmatlit, M. (2014). 42 pp (in Russian).
- [3] G.E. Abrosimova, A.S. Aronin. *Phys. Solid State* **59**, *11*, 2248 (2017).
- [4] S.M. Stishov, L.G. Khvostantsev, V.N. Slesarev, S.V. Popova, V.V. Brazhkin, et al. *Phys.-Usp.* **51**, *10*, 1055 (2008).
- [5] S.V. Popova, V.V. Brazhkin, T.I. Dyuzheva. *Phys.-Usp.* **51**, *10*, 1064 (2008).
- [6] S.M. Stishov. *Fazovye perekhody dlya nachinayushchikh. Trovant, M.*, (2014). 90 pp (in Russian).
- [7] V.F. Degtyareva, Doctoral Dissertation in Mathematics and Physics. „Struktura i ustoychivost' faz vysokogo davleniya v binarnykh splavakh *sp*-metallov“. Chernogolovka (2002). 205 pp (in Russian).
- [8] S.G. Rassolov, E.A. Sviridova, V.V. Maksimov, V.K. Nosenko, I.V. Zhikharev, D.V. Matveev, E.A. Pershina, V.I. Tkach. *Metallofiz. Noveishie Tekhnol.* **37**, *8*, 1089 (2015) (in Russian).
- [9] A.P. Shpak, V.V. Maslov, A.B. Mel'nik, A.N. Timoshevskii. *Metallofiz. Noveishie Tekhnol.* **25**, *111*, 1461 (2003) (in Russian).
- [10] V.V. Brazhkin. Candidate's Dissertation in Mathematics and Physics. „Vliyaniye vysokogo davleniya na zatverdevaniye metallicheskih rasplavov (Pb, In, Cu, dvoynye splavy na osnove medi)“. M. (1996). 150 pp (in Russian).
- [11] S.G. Menshikova, V.V. Brazhkin, V.I. Lad'yanov, B.E. Pushkarev, A.A. Suslov. *Lett. Mater.* **10**, *4*, 433 (2020).
- [12] S.G. Menshikova, V.V. Brazhkin, V.I. Lad'yanov, B.E. Pushkarev. *Crystal Growth* **524**, 125164 (2019).
- [13] S.G. Menshikova, I.G. Shirinkina, I.G. Brodova, V.V. Brazhkin, V.I. Lad'yanov, B.E. Pushkarev. *J. Crystal Growth* **525**, 125206 (2019).
- [14] I.G. Brodova, P.S. Popel', N.M. Barbin, N.A. Vatolin. *Iskhodnye rasplavy kak osnova formirovaniya strukturnykh svoystv alyuminievykh splavov*. Ural. Otd. Ross. Akad. Nauk, Yekaterinburg (2005). 369 pp (in Russian).